AD-A056 938 NAVAL OCEAN SYSTEMS CENTER SAN DIEGO CA F/G 9/3
DETECTION OF SINUSOIDS IN WHITE NOISE BY ADAPTIVE LINEAR PREDIC--ETC(U)
NOV 77 P M REEVES

UNCLASSIFIED NOSC/TR-180 NL

1 OF 1
AD
A056 938

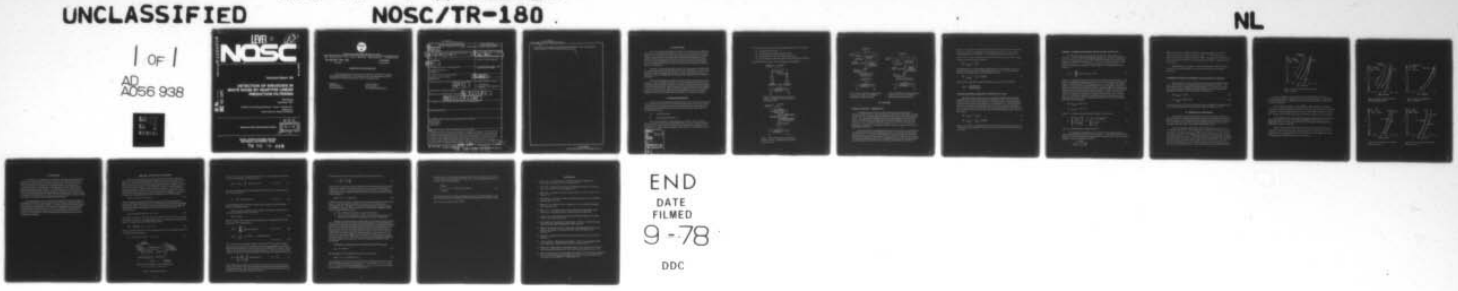

END
DATE
FILMED
9-78
DDC

LEVEL II

(12)

NOSC

NOSC TR 180

NOSC TR 180

Technical Report 180

DETECTION OF SINUSOIDS IN WHITE NOISE BY ADAPTIVE LINEAR PREDICTION FILTERING

PM Reeves

November 1977

Research and Development Report: January - October 1977

Prepared for
Naval Electronic Systems Command

NAVAL OCEAN SYSTEMS CENTER
SAN DIEGO, CALIFORNIA 92152

NAVAL OCEAN SYSTEMS CENTER, SAN DIEGO, CA 92152

AN ACTIVITY OF THE NAVAL MATERIAL COMMAND

RR GAVAZZI, CAPT, USN
Commander

HL BLOOD
Technical Director

ADMINISTRATIVE INFORMATION

The work reported here was performed from January to October 1977 under the sponsorship of NAVELEX 320. It was conducted as part of Program Element 62711N, Task Area XF11101100, Project Number F11101, Task Number 100.

Released by
RH Hearn, Head
Electronics Division

Under authority of
DA Kunz, Head
Fleet Engineering Department

UNCLASSIFIED

SECURITY CLASSIFICATION OF THIS PAGE (When Data Entered)

REPORT DOCUMENTATION PAGE

READ INSTRUCTIONS BEFORE COMPLETING FORM

1. REPORT NUMBER: NOSC/TR-180	2. GOVT ACCESSION NO. / 3. RECIPIENT'S CATALOG NUMBER
4. TITLE (and Subtitle): DETECTION OF SINUSOIDS IN WHITE NOISE BY ADAPTIVE LINEAR PREDICTION FILTERING	5. TYPE OF REPORT & PERIOD COVERED: Research and Development Jan[illegible] - Oct[illegible]77 / 6. PERFORMING ORG. REPORT NUMBER
7. AUTHOR(s): R.M. Reeves	8. CONTRACT OR GRANT NUMBER(s)
9. PERFORMING ORGANIZATION NAME AND ADDRESS: Naval Ocean Systems Center, San Diego, CA	10. PROGRAM ELEMENT, PROJECT, TASK AREA & WORK UNIT NUMBERS
11. CONTROLLING OFFICE NAME AND ADDRESS: Naval Electronic Systems Command, Washington, DC	12. REPORT DATE: November [illegible]977 / 13. NUMBER OF PAGES: 14
14. MONITORING AGENCY NAME & ADDRESS (if different from Controlling Office)	15. SECURITY CLASS. (of this report): UNCLASSIFIED / 15a. DECLASSIFICATION/DOWNGRADING SCHEDULE

16. DISTRIBUTION STATEMENT (of this Report)

Approved for public release; distribution unlimited.

16 F11101

17 XF111011100

17. DISTRIBUTION STATEMENT (of the abstract entered in Block 20, if different from Report)

18. SUPPLEMENTARY NOTES

19. KEY WORDS (Continue on reverse side if necessary and identify by block number)

Signal processing
Fourier transforms
Adaptive filters

20. ABSTRACT (Continue on reverse side if necessary and identify by block number)

This report describes four receivers for the detection of a sinusoid of known frequency but unknown phase in Gaussian white noise of known spectrum level. These are: the likelihood ratio detector, a processor employing incoherently averaged Discrete Fourier Transforms (DFTs) of the received signal, and two systems utilizing the frequency response of adaptive Linear Predictive Filters (LPFs). The LPF systems are described in detail, and an expression for optimal adaptive filter parameter selection is derived. Power curves for the four receivers are derived and compared. Results indicate that the adaptive methods are similar in performance to the incoherent DFT processor with one of the adaptive techniques offering a 1-dB reduction in input signal-to-noise ratio (SNR) for

next page

393 159

DD FORM 1 JAN 73 1473 EDITION OF 1 NOV 65 IS OBSOLETE S/N 0102-LF-014-6601

UNCLASSIFIED

SECURITY CLASSIFICATION OF THIS PAGE (When Data Entered)

78 06 29 048

20. (cont). operation at the same detection and false alarm probabilities. All three of these detectors require substantially higher SNRs than the likelihood ratio detector.

I. INTRODUCTION

The use of an adaptive linear predictive filter to detect the presence of a sinusoid in white noise has been discussed by Widrow *et al.* (Ref. 1) in a comparison of two detection methods. The first uses as its test statistic the frequency response magnitude of an adaptive linear predictive filter (LPF), the second employs incoherently averaged discrete Fourier transforms (DFTs) of the input data. Widrow's comparison is based on output signal-to-noise figures-of-merit (FOM) for the two processors and indicates that the LPF technique may offer significant improvement over the DFT when incoherent averaging is required to process the available data.

Tufts (Ref. 2) has challenged Widrow's analysis on the grounds that the DFT should have been allowed to process the data coherently. In their reply, Widrow *et al.* (Ref. 3) have agreed that a detector utilizing a coherent DFT of the data would indeed perform better than the LPF detector and suggested that a different FOM is appropriate for describing LPF performance.

Despite this interchange, the fundamental question of detector performance remains unresolved. Analysis published to date (Ref. 1) is based on FOM arguments, and these can be misleading when used in the comparison of processors with different statistical properties. In order to provide a definitive answer, the problem should be addressed from the standpoint of decision theory (Refs. 4,5). This paper represents a further step toward defining the performance of detectors utilizing LPFs by first extending Widrow's analysis to account for adaptation of the LPF, then using statistical decision theory to determine performance.

II. PROBLEM DESCRIPTION

The detection of a sinusoid in Gaussian white noise is to be considered. The frequency of the sinusoid, f_s, total noise power, σ^2, and noise power per hertz, σ_1^2, are known. Phase and amplitude of the sinusoid are unknown, but are constant over the observation interval. Each detector is to observe the data over a fixed interval, then decide which of the two possible hypotheses is true:

H_0 – noise alone present

H_1 – sine wave and noise present.

The *a priori* probabilities of these hypotheses are unknown. Hence, a Neyman-Pearson test (Ref. 4) will be used to decide whether H_0 or H_1 is true. A scalar test statistic generated by each detector will be compared to a fixed threshold for that detector. The threshold is set to achieve a desired probability of false alarm (*i.e.*, the probability of choosing H_1 when H_0 is true).

Four detector structures described in the following section are to be considered:

(1) The optimal detector (Fig. 1).

(2) Averaged spectral estimates of the data (Fig. 2).

(3) Fourier transform of the LPF weight vector (Fig. 3).

(4) Fourier transform magnitude squared of the LPF weight vector (Fig. 4).

The predictive filters of Figs. 3 and 4 are described in the Appendix.

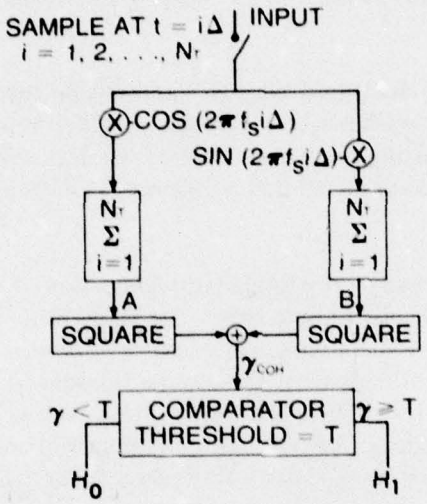

Figure 1. Coherent DFT detector for a sinusoid of frequency f_s in bandlimited Gaussian white noise of known spectrum level.

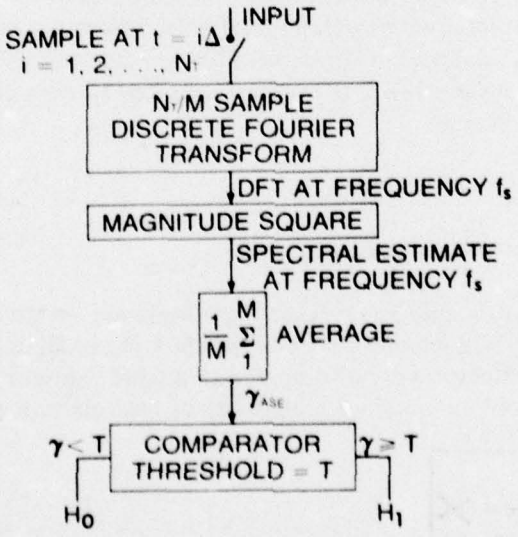

Figure 2. Averaged spectral estimate (ASE) detector for a sinusoid of frequency f_s in bandlimited Gaussian noise of known spectrum level.

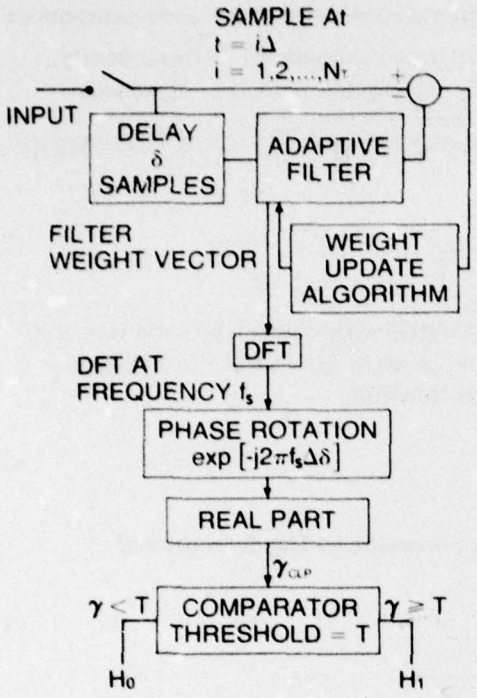

Figure 3. Coherent linear predictor (CLP) detector for a sinusoid of frequency f_s in bandlimited Gaussian noise of known spectrum level.

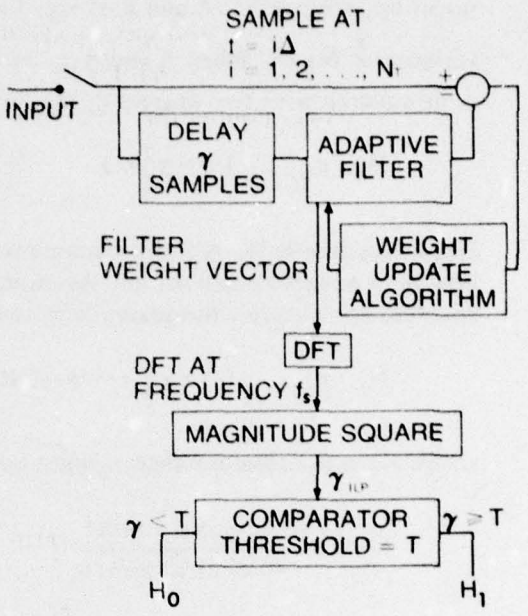

Figure 4. Incoherent linear predictor (ILP) detector for a sinusoid of frequency f_s in bandlimited Gaussian noise of known spectrum level.

III. ANALYSIS

OPTIMAL DETECTOR – COHERENT DFT

The likelihood ratio detector for a signal of unknown amplitude and phase is discussed by Helstrom (Ref. 5). This optimal detector, which is the coherent DFT mentioned by Tufts (Ref. 2), can be implemented by splitting the input data into two channels as shown in Fig. 1. The first channel is multiplied by $\cos(2\pi f_s t)$ and integrated over the observation interval. The second channel is multiplied by $\sin(2\pi f_s t)$ and integrated. At the end of the observation period a test statistic, denoted by γ_{COH} in Fig. 1, is formed by squaring and summing the two integrals. The Neyman-Pearson test is applied to γ_{COH} in order to decide signal presence or absence.

One practical method of implementing this detector uses the DFT. The observed data are sampled at Nyquist rate and the resulting data sequence is transformed with the known sinusoid frequency, f_s, at one of the DFT frequencies. Real and imaginary parts of the DFT at this frequency are squared and summed to form the test statistic. Note that the data must be transformed coherently. That is, either a single DFT must process the entire data sequence in one transformation, or short DFTs can be summed in phase before the test statistic is

formed. Let N_T denote the total number of data samples processed. The noise component of the data is assumed Gaussian with zero mean and known variance σ^2. Consequently, under hypotheses H_0, A and B of Fig. 1 are normally distributed with zero mean and variance $\frac{1}{2} N_T \sigma^2$. When A and B are normalized to unit variance, the test statistic, γ_{COH}, is chi-squared with two degrees of freedom:

$$H_0 : p_{\gamma_{COH}}(\cdot) = \chi^2_2(\cdot) \tag{1}$$

Under hypothesis H_1 A and B remain normally distributed with unchanged variances, but now have nonzero mean values. Assuming normalization as in Eq. (1), the test statistic becomes non-central chi-squared with two degrees of freedom:

$$H_1 : p_{\gamma_{COH}}(\cdot) = \chi^{2'}_2(\cdot | N_T SNR), \tag{2}$$

where N_T is the total number of input data samples processed by the detector and

$$SNR = \frac{\text{sinusoid power}}{\text{total noise power}} \tag{3}$$

AVERAGED SPECTRAL ESTIMATES OF THE INPUT DATA (ASE)

The optimal detector may require an extraordinarily long DFT if the input time-bandwidth product is large and DFTs cannot be summed coherently. When the optimal detector is not practical for a given application, a sub-optimal detector employing averaged spectra of the input data sequence may be used. As illustrated in Fig. 2, the test statistic is forming by summing the squared absolute values of short, non-overlapping (independent) DFTs. As in the case of the optimal detector, f_s must correspond to the center frequency of one of the DFT frequency bins. The test statistic probability distributions under hypotheses H_0 and H_1 are

$$H_0 : p_{\gamma_{ASE}}(\cdot) = \chi^2_{2m}(\cdot) \tag{4}$$

$$H_1 : p_{\gamma_{ASE}}(\cdot) = \chi^{2'}_{2m}(\cdot | N_T SNR), \tag{5}$$

where m is the number of independent DFTs used in forming the test statistic, and N_T, the total number of data samples processed, is equal to m times the number of samples processed by each DFT.

COHERENT FOURIER TRANSFORM OF THE LPF WEIGHT VECTOR (CLP)

The LPF used in this work is discussed in the Appendix. The weight vector is modeled as a sinusoid of time-varying amplitude summed with a Gaussian "misadjustment" noise. Equations (22), (23), (25), and (26) describe the LPF weight vector, W(i,k), where i denotes the individual weight number ($0 < i < N-1$) and k denotes the number of adaptation iterations ($k = 1,2, \cdots$). The CLP detector (Fig. 3) uses as its test statistic the measured amplitude of the weight vector cosine component. This amplitude is estimated by the sum

$$\gamma_{CLP} = \sum_{i=0}^{N-1} W(i,k) \cos[2\pi f_s (i + \delta)\, \Delta], \tag{6}$$

where f_s is the sinusoid frequency to be detected, δ is the LPF prediction delay (Fig. 3), and Δ is the sampling period of the digital system. The test statistic is computed, as illustrated in Fig. 3, by first forming the DFT of the weight vector (i.e., evaluating the LPF frequency response at frequency f_s), then rotating the phase of this complex quantity as indicated. The real part of the result is used as the test statistic. Since the weight vector misadjustment noise is assumed to be Gaussian, the test statistic will also be Gaussian. The variance of the misadjustment, and hence the variance of the test statistic, is constant under H_0 and H_1. In the present analysis it is assumed that all weights are initially set to zero (i.e., $W(i,0) = 0$, $0 < i < N-1$) and that a single DFT is calculated at the end of the observation period. When normalized to unit variance, the probability distributions of the test statistic under H_0 and H_1 are (see Appendix)

$$H_0 : p_{\gamma_{CLP}}(\cdot) = N(\cdot \mid 0,1) \tag{7}$$

$$H_1 : p_{\gamma_{CLP}}(\cdot) = N(\cdot \mid \alpha,1), \tag{8}$$

where $N(\cdot \mid x,y)$ denotes the normal density with mean x and variance y,

$$\alpha = \left[\frac{\frac{N}{2}\,SNR}{1 + \frac{N}{2}\,SNR}\right] \frac{1 - [1 - 2\mu\sigma^2(1 + \frac{N}{2}\,SNR)]^{N_T}}{\left[\frac{N}{2}\,\mu\sigma^2\right]^{1/2}}, \tag{9}$$

and μ is the adaptive feedback constant of the LPF.

The probability of sinusoid detection can be maximized by separating the test statistic distributions under H_0 and H_1 as far as possible, *i.e.*, choosing the controllable LFP parameters N and μ so as to make α as large as possible. Assuming N to be fixed by hardware limitations, this is accomplished by choosing

$$\mu = \frac{1.25643}{2\sigma^2 N_T (1 + \frac{N}{2}\,\hat{SNR})}. \tag{10}$$

$\hat{SNR}$ is a nominal value of SNR to be detected, and the numerator of Eq. (10) is the nonzero root of the transcendental equation $(1 + 2x)e^{-x} = 1$. With this choice of μ, detector performance is optimized when SNR = $\hat{SNR}$. Curves presented in Section IV will show that detector performance is not strongly influenced by $\hat{SNR}$, and therefore its value is not critical.

Substituting Eq. (10) into Eqs. (9) and (8) gives the density of the test statistic as a function of N, N_T, SNR, and $\hat{SNR}$. These parameters determine the CLP detector performance.

INCOHERENT FOURIER TRANSFORM OF THE LPF WEIGHT VECTOR (ILP)

This detector (Fig. 4) does not utilize the deterministic phase of the LPF weight vector. The test statistic is the magnitude squared of the weight vector DFT (*i.e.*, the LPF frequency response magnitude squared) at frequency f_s. The model of the weight vector is developed in the Appendix. Probability densities of the test statistic under hypotheses H_0 and H_1 are (with normalization to unit variance)

$$H_0 : p_{\gamma_{ILP}}(\cdot) = \chi^2_2(\cdot) \tag{11}$$

$$H_1 : p_{\gamma_{ILP}}(\cdot) = \chi^{2'}_2(\cdot|\alpha^2), \tag{12}$$

where α is given by Eq. (9). Just as for the CLP detector, probability of sinusoid detection is maximized by choosing the adaptive feedback constant according to Eq. (10).

IV. PERFORMANCE COMPARISONS

The density functions of Section III will now be used to develop comparisons of detector performance. Results are based on the Neyman-Pearson hypothesis test and are in the form of power curves showing detection probabilities as a function of false alarm probability and SNR of the received signal. The plots published by Marcum (Ref. 6) and the nomogram of Urkowitz (Ref. 7) were used in obtaining these curves.

Figure 5 compares the coherent DFT, ASE, and ILP detectors for the case of 102,400 input data samples. The ASE DFT length of 1024 points was chosen to equal the LPF weight vector length. The parameter $\hat{SNR}$ required in order to choose μ for the ILP was selected equal to 1×10^{-3} (–30 dB). Figure 5 shows that the ILP and ASE processors are roughly equal in performance. The ILP offers a fraction of a dB advantage at the higher SNR values shown, but the ASE performs slightly better at smaller SNRs. This result differs from the conclusion of Widrow's analysis (Ref. 1) based on a FOM comparison which indicated a large difference between the ASE and ILP processors. As predicted by Tufts (Ref. 2), the coherent DFT detector is markedly better than either the ASE or ILP detectors.

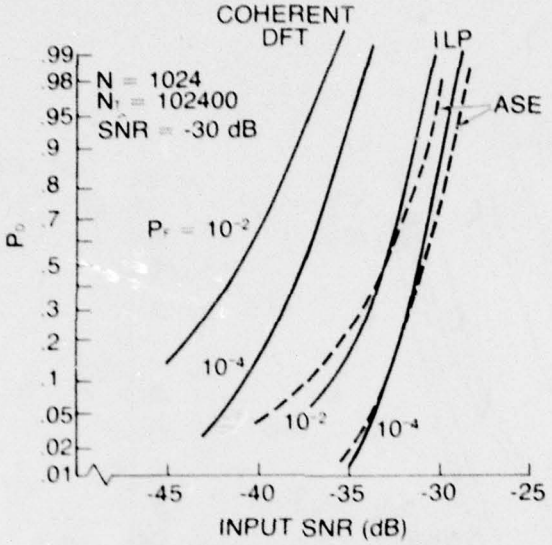

Figure 5. Comparison of coherent DFT, ILP, and ASE detector performance.

Figure 6 compares the coherent DFT, ASE, and CLP detectors for the case of 102,400 input data samples. All parameters are the same as those of Fig. 5. Figure 6 shows that the CLP offers about a 1-dB improvement over the ASE processor, but is still far short of optimal performance.

Figure 7 illustrates the effect of varying $\hat{SNR}$ on CLP performance. The change in performance is negligible as $\hat{SNR}$ is reduced from 10^{-3} to 10^{-4}. The SNR required to achieve a given P_D in the range illustrated increases only about 3 dB as $\hat{SNR}$ is increased from 10^{-3} to 10^{-2}. Thus the choice of $\hat{SNR}$ is not critical to LPF detector performance in this example.

Figure 8 shows the effect of varying the weight vector length of the CLP detector and DFT length of the ASE detector. The relative performance of the two detectors is not significantly affected. In both cases the CLP detector offers about a 1-dB advantage in the SNR required to achieve a given P_D.

Figure 9 compares ASE and CLP detector performance for two values of N_T, the total number of data samples processed. Relative performance of the two processors is not strongly affected. At the smaller value of N_T, the CLP detector offers slightly more than a 1-dB advantage in the SNR required to achieve a given P_D.

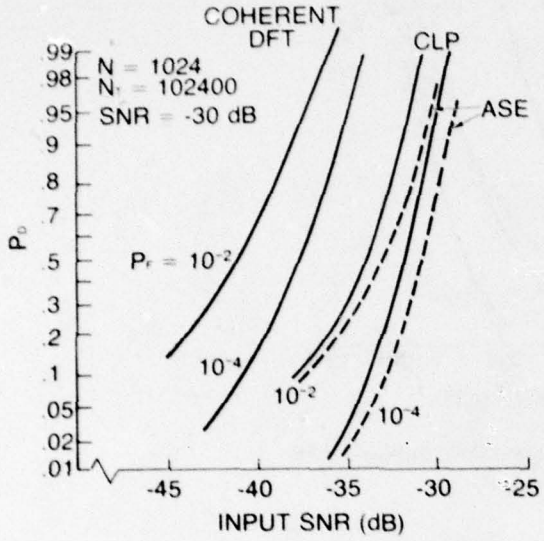

Figure 6. Comparison of coherent DFT, ASE, and CLP detector performance.

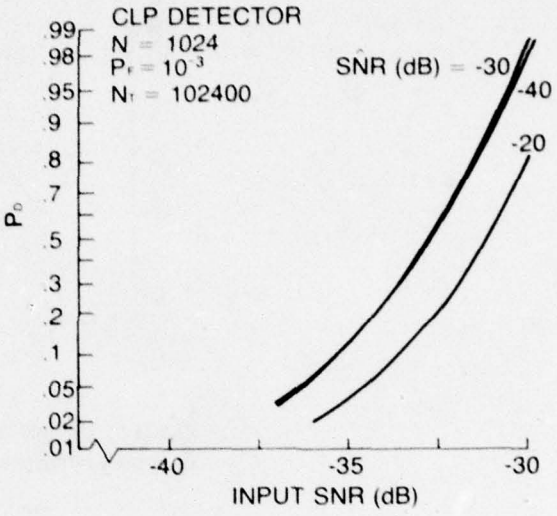

Figure 7. Effect of varying $\hat{SNR}$ on CLP detector performance.

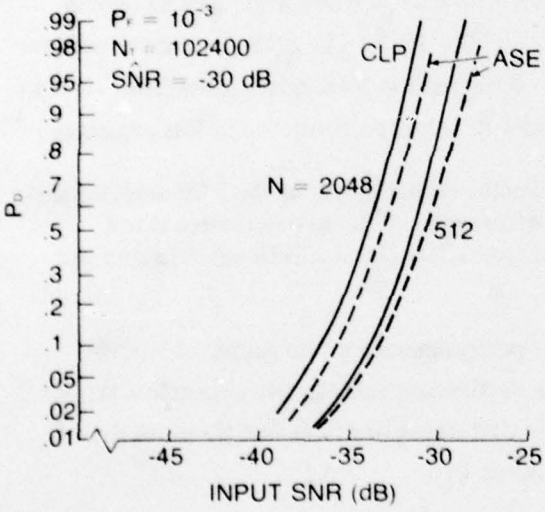

Figure 8. Effect of varying N on CLP and ASE detector performance.

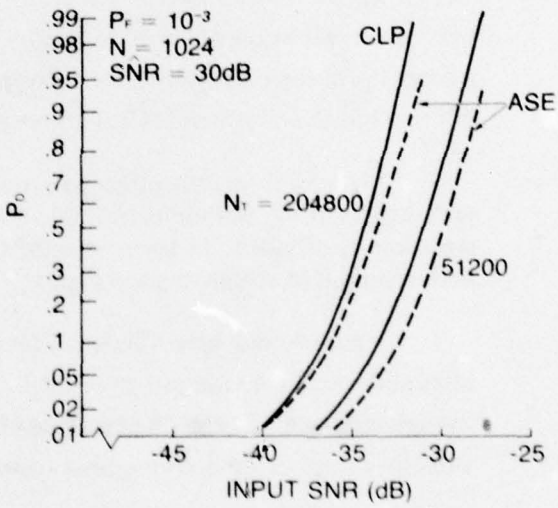

Figure 9. Effect of varying N_T on CLP and ASE detector performance.

V. CONCLUSIONS

Four detectors of a sinusoid of known frequency in Gaussian white noise have been analyzed. Two of these utilized the frequency response of an adaptive linear predictive filter, and two employed Fourier transforms of the input data. The results show that the CLP processor (Fig. 3), which utilizes the deterministic phase of the LPF frequency response, offers about a 1-dB advantage over the ASE detector, which utilizes averaged spectral estimates of the input data (Fig. 2). The ILP detector (Fig. 4), which does not utilize the LPF phase, performs about the same as the ASE detector. The ASE, ILP, and CLP detectors all require significantly higher SNR than the optimal detector, which employs a coherent DFT of the input data. In all cases, the CLP and ILP adaptive feedback constants were chosen to yield the best possible adaptive filter performance.

The work presented here has treated the use of adaptive LPF frequency response as a method of signal detection. Spectral analysis of the LPF output, discussed by Zeidler and Chabries (Ref. 9), is an alternative technique. It should be noted that the detection problem treated in this paper assumed that the receiver had a considerable amount of information concerning both the signal and noise characteristics. As suggested by Griffiths (Ref. 10), conditions of greater signal uncertainty (e.g., nonstationary noise or non-white noise of unknown spectral density) may result in adaptive processor performance superior to that of nonadaptive techniques.

APPENDIX: LPF WEIGHT VECTOR MODEL

Figure 10 illustrates the linear predictor considered in this report. A thorough discussion of this system (also known as the adaptive line enhancer) has been presented by Widrow *et al.* (Ref. 1) and Treichler (Ref. 11). Only a brief summary is given here. The adaptive filter of Fig. 10 is a time domain digital filter which adjusts its impulse response so as to minimize the mean square of ϵ, the difference between the desired filter response, x, and its actual response, y. When the filter adjustment is complete, y approximates the minimum mean square error prediction of x over the interval of δ samples. For the analysis which follows, it is assumed that x is statistically stationary and composed of a sine wave in white noise. The updating algorithm for the k^{th} iteration of the i^{th} filter weight is

$$W(i,k+1) = W(i,k) + 2\mu\epsilon(k)\, x(i,k) \tag{13}$$

where x(i,k) is the data sample at the i^{th} filter tap during the k^{th} iteration and W(i,k) denotes the i^{th} weight at the k^{th} iteration. The constant μ controls the feedback magnitude of the adaptive system. For stability, μ must be chosen greater than zero and smaller than the reciprocal of the largest eigenvalue of the input data correlation matrix, $\underset{\sim}{R}$. The elements of $\underset{\sim}{R}$ are

$$R_{mn} = E_k\,[x(m,k)\, x(n,k)]\,,\ 0 < m,n < N-1\ , \tag{14}$$

where R_{mn} is the element in the m^{th} row and n^{th} column, and $E_k\,[\cdot]$ denotes expectation with respect to the index k. The optimal LPF weight vector, resulting in the minimum mean square of ϵ, is given by the discrete Wiener-Hopf equation:

$$W(i) = \left[R^{-1}\right]_{ik}\ P_k,\quad 0 < i,k < N-1\ , \tag{15}$$

where P_k is the k^{th} component of P, the correlation vector of the desired filter response and the data contained in the filter, *i.e.*,

$$P_k = E_m[x(-\delta,m)\, x(k,m)]\,.\quad 0 < k < N-1 \tag{16}$$

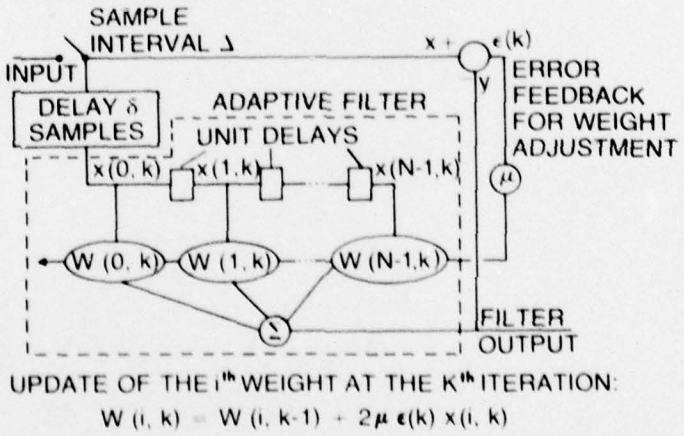

Figure 10. The adaptive linear predictor.

For the case of a sine wave of magnitude A and frequency f_s in white noise of total power σ^2 in the input bandwidth, the elements of $\underline{R}$ are

$$R_{mn} = \sigma^2\delta_{mn} + \frac{A^2}{2}\cos[2\pi f_s (m-n)\,\Delta] \qquad 0 \le m,n \le N-1, \tag{17}$$

where Δ is the sampling period of the digital LPF system and δ_{mn} is the Kronecker delta. The components of $\underline{P}$ are

$$P_m = \frac{A^2}{2}\cos[2\pi f_s (m+\delta)\,\Delta] \qquad 0 \le m \le N-1. \tag{18}$$

In the following it will be convenient to assume that f_s is neither zero nor the Nyquist frequency of the digital system.

Since f_s is known, Δ and the predictor weight vector length, N, can be chosen to equal an integer number of sine wave periods.

$$f_s \Delta N = \text{integer} \tag{19}$$

When N is chosen in this way $\underline{R}$ becomes circulant (Ref. 8). The eigenvalues, $\lambda^{(m)}$, and eigenvectors, $\underline{U}^{(m)}$, of $\underline{R}$ are given by

$$\lambda^{(m)} = \sum_{n=0}^{N-1} R_{0n} \exp[-j2\pi mn/N] \qquad 0 \le m \le N-1 \tag{20}$$

$$\underline{U}^{(m)} = \frac{1}{\sqrt{N}}\,[1, e^{-j2\pi m/N}, \ldots, e^{-j2\pi m(N-1)/N}]^T \qquad 0 \le m \le N-1, \tag{21}$$

where T denotes vector transpose. Note that $\underline{U}^{(m)}$ and $\underline{U}^{(N-m)}$ are complex conjugates. The eigenvectors are complex exponentials, each with an integral number of cycles in the length of the LPF weight vector. Because N has been appropriately chosen and f_s is suitably restricted, two of the eigenvectors correspond to frequency f_s. Equation (15) can be solved using Eqs. (20) and (21). The optimal weight vector is found to be a sinusoid of frequency f_s:

$$W(i) = \left[\frac{SNR}{1 + \frac{N}{2}SNR}\right]\cos[2\pi f_s (i+\delta)\,\Delta] \qquad 0 \le i \le N-1 \tag{22}$$

where SNR denotes the sinusoid to noise power ratio. This is the form to which the LPF weight vector would converge, given an infinitely long adaptation interval and the absence of misadjustment noise. The optimum weight vector is orthogonal to all but the two conjugate eigenvectors of $\underline{R}$ which correspond to frequency f_s.

The eigenvalues associated with these eigenvectors are equal and are given by

$$\lambda = \sigma^2 \left(1 + \frac{N}{2} SNR\right). \tag{23}$$

Treichler (Ref. 11) has shown that these eigenvalues control the speed with which the LPF weight vector converges to its optimal value. They are inversely proportional to the convergence time constant. Assuming the weight vector to be initially zero, and neglecting transient behavior as the predictor initially fills with data, the mean value of the i^{th} weight at the k^{th} update is

$$W(i,k) = [1 - (1 - 2\mu\lambda)^k]\, W(i). \tag{24}$$

In addition to this mean value, the weight vector also contains misadjustment noise. Widrow (Refs. 1, 12) has shown that the mean value of this noise is zero, and its variance is approximated by $\mu\sigma^2$. Misadjustment is uncorrelated from weight to weight. In order to extend Widrow's analysis of detector performance, the following two assumptions will be made concerning misadjustment noise:

(1) The misadjustment distribution is approximately normal.

(2) Variance of the misadjustment is equal to the steady-state value of $\mu\sigma^2$ at all times, and is not influenced by the presence or absence of the sinusoid.

Reference 13 presents data from extensive Monte Carlo experiments with the system of Fig. 10. These show that the steady state weight misadjustment is normally distributed when the filter is driven by uncorrelated Gaussian input samples. The results presented in this paper are for uncorrelated Gaussian input plus a sinusoid of less than -20 dB relative noise power. The presence of the sinusoid would therefore seem to be unimportant insofar as misadjustment is concerned. In addition, the optimal value of μ (Eq. 10) can be shown to imply that the observation interval of N_T input data samples is equal to about 1.26 convergence time constants when $\widehat{SNR}$ is near the true SNR. Convergence is therefore about 70 percent complete. In view of this, the use of the steady state misadjustment distribution and variance assumed here would seem to provide a reasonable representation of filter misadjustment.

Under the above assumptions, the noise component of the i^{th} LPF weight is

$$p_{\eta_i} = N(\cdot 10, \mu\sigma^2). \tag{25}$$

The LPF weight vector is modeled by the sum of Eqs. (24) and (25):

$$W(i,k) = [1 - (1 - 2\mu\lambda)^k]\, W(i) + \eta_i \tag{26}$$

In working with Eq. (26) it is convenient to note that, for the situations of interest in this paper, the square-bracketed term is of the form $[1 - (1-x)^y]$, where $x << 1$, $y >> 1$, and $x^2 y << 1$. This term is closely approximated by $[1 - e^{-xy}]$, as can be shown by taking the natural logarithm of $(1 - x)^y$ and expanding in powers of x.

Substituting Eq. (22) for W(i) and evaluating the DFT of Eq. (26) at frequency f_s results in a complex number with deterministic and random parts. The deterministic part is due to the first term of Eq. (26) and is equal to

$$\frac{\frac{N}{2}SNR}{1+\frac{N}{2}SNR}[1-(1-2\mu\lambda)^k]\exp[j\,2\pi\,f_s\,\delta\Delta]\ . \tag{27}$$

The random part is due to the noise component of Eq. (26). The real and imaginary components of the random part are independent, identically distributed normal random variables with zero mean and variance equal to $\frac{N}{2}\mu\sigma^2$.

REFERENCES

1. Widrow, B., *et al;* "Adaptive Noise Cancelling: Principles and Applications," *Proceedings of IEEE*, Vol. 63, No. 12, December 1975.

2. Tufts, D. W., "Adaptive Line Enhancement and Spectrum Analysis," *Proceedings of IEEE*, Vol. 65, No. 1, pp 169–170, January 1977.

3. Widrow, B., *et al;* Reply to Tufts, *Proceedings of IEEE*, Vol. 65, No. 1, pp 171–173, January 1977.

4. Van Trees, H. L., *Detection, Estimation, and Modulation Theory, Part 1*, John Wiley and Sons, New York, 1968.

5. Helstrom, C. W., *Statistical Theory of Signal Detection*, Second Edition, Pergargon Press, New York, 1968.

6. Marcum, J. I., "A Statistical Theory of Target Detection by Pulsed Radar," *IRE Transactions on Information Theory*, Vol. IT-6, pp 59–267, April 1960.

7. Urkowitz, H., "Energy Detection of Unknown Deterministic Signals," *Proceedings of IEEE*, Vol. 55, No. 4, April 1967.

8. Gray, Robert M., "Toeplitz and Circulant Matrices: A Review," Stanford University Center for Systems Research Report SEL-71-032, June 1971.

9. Zeidler, J. R. and Chabries, D. M., "An Analysis of the LMS Adaptive Filter used as a Spectral Line Enhancer," Naval Undersea Center Technical Publication 556, February 1975.

10. Griffiths, L. J., Reply to Tufts, *Proceedings of the IEEE*, Vol. 65, No. 1, pp 170-171, January 1977.

11. Treichler, John R., "The Spectral Line Enhancer – The Concept, an Implementation, and an Application," PhD dissertation, Stanford University, June 1977.

12. Widrow, B., "Adaptive Filters," appearing in *Aspects of Network and System Theory*, edited by Kalman and DeClaris, New York: Holt, Rinehart, and Winston, Inc., 1970.

13. Rockwell International, "Transverse Adaptive Filter March 1978," Rockwell International Electronic Systems Group report C78-407/301 prepared for the Naval Ocean Systems Center under contract N66001-77-C-0408, March 1978.